arXiv:1101.1175v1 [cond-mat.supr-con] 6 Jan 2011

[35]**********

A slightly shortened version of this paper is published in

Phys. Rev. Lett. **106**, 017002 (2011)

http://link.aps.org/doi/10.1103/PhysRevLett.106.017002

This file includes also the supplementary material - starting on page 11 here

http://link.aps.org/supplemental/10.1103/PhysRevLett.106.017002

****

Observation of two Andreev-like energy scales in $La_{2-x}Sr_xCuO_4$ superconductor/normal-metal/superconductor junctions

G. Koren* and T. Kirzhner

Physics Department, Technion - Israel Institute of Technology Haifa, 32000, ISRAEL†

(Dated: January 7, 2011)

Abstract

Conductance spectra measurements of highly transparent ramp-type junctions made of superconducting $La_{2-x}Sr_xCuO_4$ electrodes and non superconducting $La_{1.65}Sr_{0.35}CuO_4$ barrier are reported. At low temperatures below T_c, these junctions have two prominent Andreev-like conductance peaks with clear steps at energies Δ_1 and Δ_2 with $\Delta_2 > 2\Delta_1$. No such peaks appear above T_c. The doping dependence at 2 K shows that both Δ_1 and Δ_2 scale roughly as T_c. Δ_1 is identified as the superconducting energy gap, while a few scenarios are proposed as for the origin of Δ_2.

PACS numbers: 74.45.+c, 74.25.F-, 74.25.Dw, 74.72.-h

*Electronic address: gkoren@physics.technion.ac.il

†URL: `http://physics.technion.ac.il/~gkoren`

The issue of two distinct energy gaps in the cuprates has been discussed by many authors, and the question whether both are related to superconductivity is still controversial [1–4]. In one scenario, one energy gap is the coherence gap which opens at T_c with the onset of phase coherent superconductivity, while the other gap opens at T^* which marks the cross over to the pseudogap regime and possibly the creation of uncorrelated pairs [5]. In contrast to this scenario, some ARPES measurements show only a single energy gap, which indicate that the superconducting gap and the pseudogap might be the same entity [6, 7]. In another scenario, the regime above T_c in the underdoped cuprates which exhibits a signature of the condensate, can be attributed to strong superconducting fluctuations. This behavior was found in measurements of the Nernst effect [8], whose T_c(onset) values scale with doping roughly as the superconducting dome. This effect therefore, is related to T_c and apparently depends on more than one energy scale of the condensate. Previous point contact measurements of tunneling and Andreev conductance have shown that the tunneling gap which scales as T^* is larger than the Andreev gap which follows T_c [2, 9–11]. In the present study we report on similar conductance measurements in ramp-type junctions of the $La_{2-x}Sr_xCuO_4$ (LSCOx or LSCO) system, but due to their high transparency we observe mostly Andreev gaps. Surprisingly, we find two different such gaps in this system below T_c both of which scale versus doping roughly as the superconducting dome. Only single gaps were observed in previous conductance measurements in LSCOx [10–13]. The results though show that in Refs. [10–12] the gaps follow T_c while in Ref. [13] the gaps scale as T^*. The present low energy Andreev peak in the conductance spectra is attributed to the superconducting gap, while a few scenarios are discussed in relation to the origin of the second high energy feature in the spectra.

Highly transparent superconductor - normal metal - superconductor (SNS) junctions of the cuprates can be obtained if the S electrodes and the N barrier have similar density of states and Fermi velocities. In the LSCOx system the doping levels are determined mostly by the Sr content, provided the same oxygen annealing process is used. Therefore, highly transparent junctions can be realized, if the S electrodes are in the superconducting

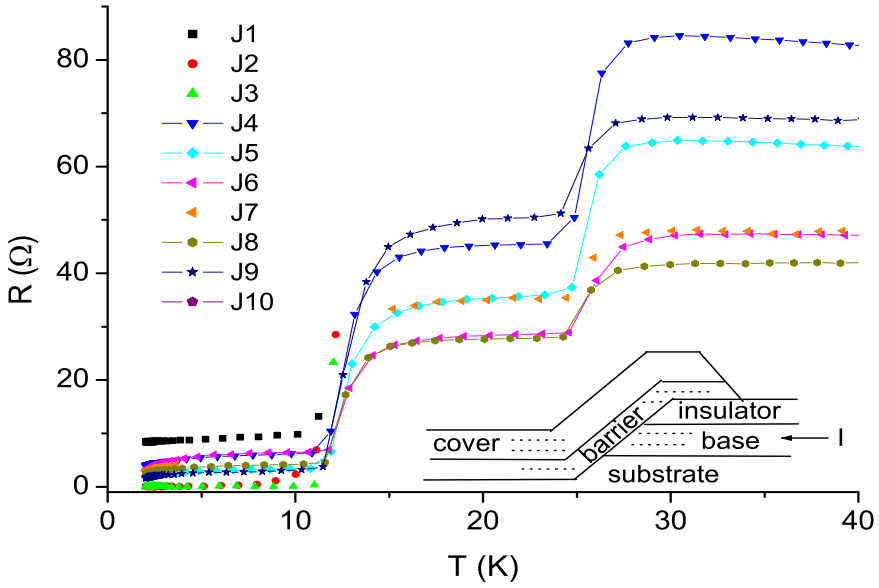

FIG. 1: Resistance versus temperature of all the LSCO10 junctions on the wafer. The inset shows a schematic drawing of a ramp-type junction, where the 77 nm thick base and cover electrodes are made of LSCOx and the 33 nm thick barrier is made of LSCO35.

regime ($0.06 \leq x \leq 0.25$) while the N barrier is non-superconducting with $x \approx 0.35 - 0.45$. This scenario however, can not be realized in the $YBa_2Cu_3O_{7-\delta}$ (YBCO) system, since one can not dope the S and N electrodes differently with two different oxygen contents in the same junction. Pr and Fe doped YBCO had been used in the past as barriers in SNS junctions [14–16], but these dopants introduce larger disturbances in the YBCO matrix as compared the different Sr doping levels in the LSCO electrodes. We thus investigated LSCOx-LSCO35-LSCOx ramp-type junctions with x values of 0.1, 0.125, 0.15 and 0.18, in order to determine the various Andreev-like gaps and study the doping dependence (or phase diagram) of these gaps. Ten junctions were prepared for each doping level along the anti-node direction in the geometry shown in the inset to Fig. 1, on 1×1 cm^2 wafers of (100) $SrTiO_3$ (STO). All the different LSCO layers were grown epitaxially with the c-axis normal to the wafer, and thus a-b plane coupling was obtained between the base and cover electrodes. All junctions had the same geometry with $5\,\mu$ width, and 77 and 33 nm films and barrier thicknesses, respectively. Typical 4-probe results of the resistance versus

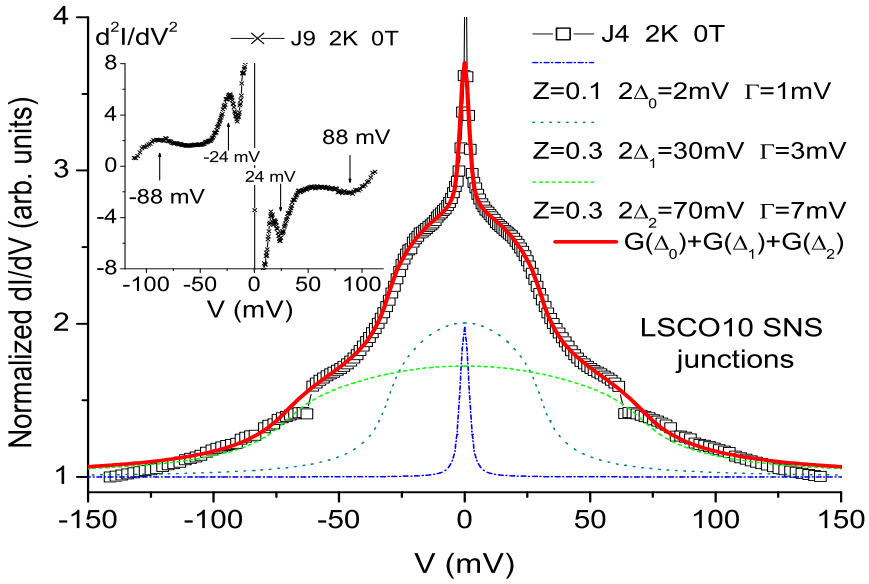

FIG. 2: Conductance spectrum of an anti-node SNS junction of LSCO10-LSCO35-LSCO10 at 2K with a fit to the BTK model for a d-wave superconductor. The three components of the fit with Δ_0, Δ_1 and Δ_2 are also shown. The inset shows the derivative of the conductance data of another junction on the same wafer.

temperature for $x = 0.1$ are shown in Fig. 1. One can easily see the two distinct transition temperature onsets at 28 and 15 K, which correspond to the T_c values of the cover and base electrodes, respectively. The reason for this is that the base electrode on the pristine STO surface is more strained than the cover electrode which is grown on a 33 nm thick LSCO35 layer on top of the ion milled area of the STO wafer [17]. Below about 10 K, the quite constant junctions resistance can be seen which ranges between $0 - 8\,\Omega$ while most junctions have $2-4\,\Omega$. Junction 10 had bad contacts while junctions 2 and 3 have critical current.

Fig. 2 shows a representative normalized conductance spectrum at 2 K of the junction J4 of Fig. 1. This spectrum has three pronounced features. The first is a narrow zero bias conductance peak (ZBCP), the second is a dome like peak of intermediate width which is superimposed on a third feature which is even broader. The conductance data is therefore the result of a sum of three components which can be written as

G(total)=$G(\Delta_0)$ + $G(\Delta_1)$ + $G(\Delta_2)$. Note that the gap feature in SNS junction always appears at 2Δ [18]. Interference phenomena such as Tomasch [19] or McMillan-Rowel [20] oscillations do not affect this gap voltage and are absent in the present study (apparently due to the very thick barrier and small ramp angle), though they had been observed previously in similar YBCO based SNS junctions [15, 21]. Furthermore, the use of interference free SN junctions with a single interface involves other problems in the determination of the voltage drop on the junctions due to the much large voltage drop of the leads [22]. We therefore decided to work with SNS junctions with possible interference effects but with zero lead resistance and accurate energy or voltage scale. We used the BTK model modified for a d-wave superconductor given by Tanaka and Kashiwaya to fit our data [23]. The three conductance components $G(\Delta_i)$ of these fits are shown in Fig. 2 together with the total conductance curve G(total) which fits the data quite well. The barrier strength Z_i, the Andreev gap parameters Δ_i and the lifetime broadening Γ_i are also given in Fig. 2. One can see that the Z_i values are quite low which indicates a highly transparent junction. This justifies our use of the anti-node direction formula without mixing of the node direction, since both are quite similar when the Z_i values are small. We also note that the maximum conductance value of each component in Fig. 2 is at around 2 which is like the expected Andreev value of the conductance of a pair for each incident electron. Although this fitting procedure involves many parameters, the clear Andreev-like gap features at Δ_1 and Δ_2 can be deduced from the raw data directly by taking the derivative of the conductance as shown in the inset. This was done for a different junction on the same wafer, and one can see that the peak locations are quite close to the different $2\Delta_i$ obtained before, but this also reflects the spread of these values on the same wafer. Additional conductance spectra that show the spread of the $2\Delta_i$ values are shown in Figs. 4S, 5S and 6S of the supplementary material for LCO15-LSCO35-LSCO15 junctions [22]. Fig. 3S there shows that the conductance spectra of LSCO10-LSCO35 SN junctions [22] are basically quite similar to the results of Fig. 2 here on SNS junctions. We note in passing that the sharp resonances at $\pm$62 mV in Fig. 2 are not very common and appear in about one out of ten junctions on a wafer.

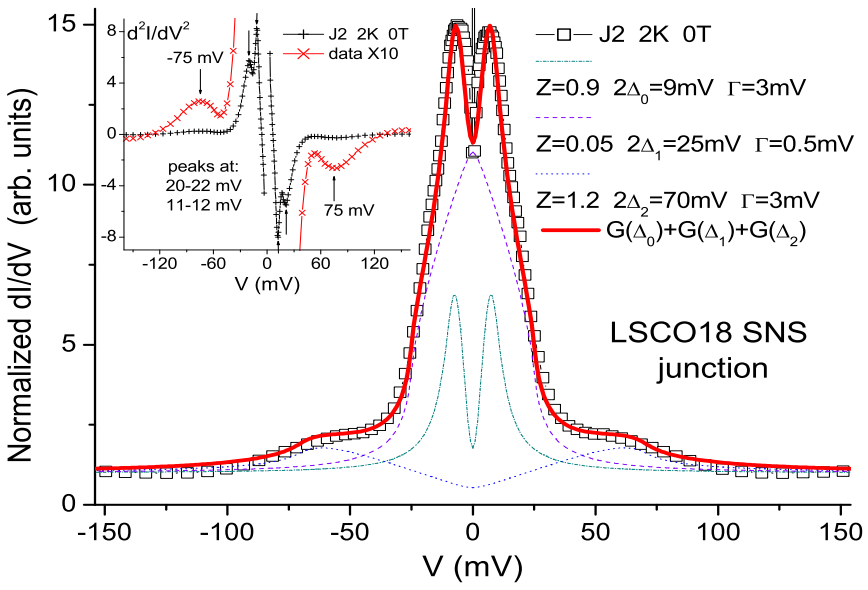

FIG. 3: Conductance spectrum of an anti-node junction of LSCO18-LSCO35-LSCO18 at 2K with a fit to the d-wave BTK model together with the three components of this fit with Δ_0, Δ_1 and Δ_2. The inset shows the derivative of the conductance data of the main panel.

A typical conductance spectrum of a LSCO18-LSCO35-LSCO18 junction at 2 K together with a fit with its three components as before are shown in Fig. 3. The dominant component contributing to this spectrum is the highly transparent one at Δ_1, but unlike in Fig. 2, its maximum value now is above 10 and not around 2. We attribute this behavior to the presence of bound states which can cause this effect [23]. The Δ_2 feature is still quite clear but has a small spectral weight as compared to that of Δ_1. It also has a lower transparency and shows a tunneling-like behavior. The third feature near zero bias now looks like a split ZBCP, again with intermediate transparency and tunneling-like behavior. The very narrow ZBCP of Fig. 2 is gone, and only a remnant critical current is observed. The inset to Fig. 3 shows the derivative of the conductance d^2I/dV^2 of the same junction. One can see that the peak energies now are even closer to those obtained from the fitting procedure in comparison to the results of Fig. 2. Fig. 4 shows a few conductance spectra of the same junction at different temperatures. As expected, both Δ_1 and Δ_2 are suppressed with increasing temperature while Δ_0 is basically unaffected. The inset to Fig. 4 (b) shows

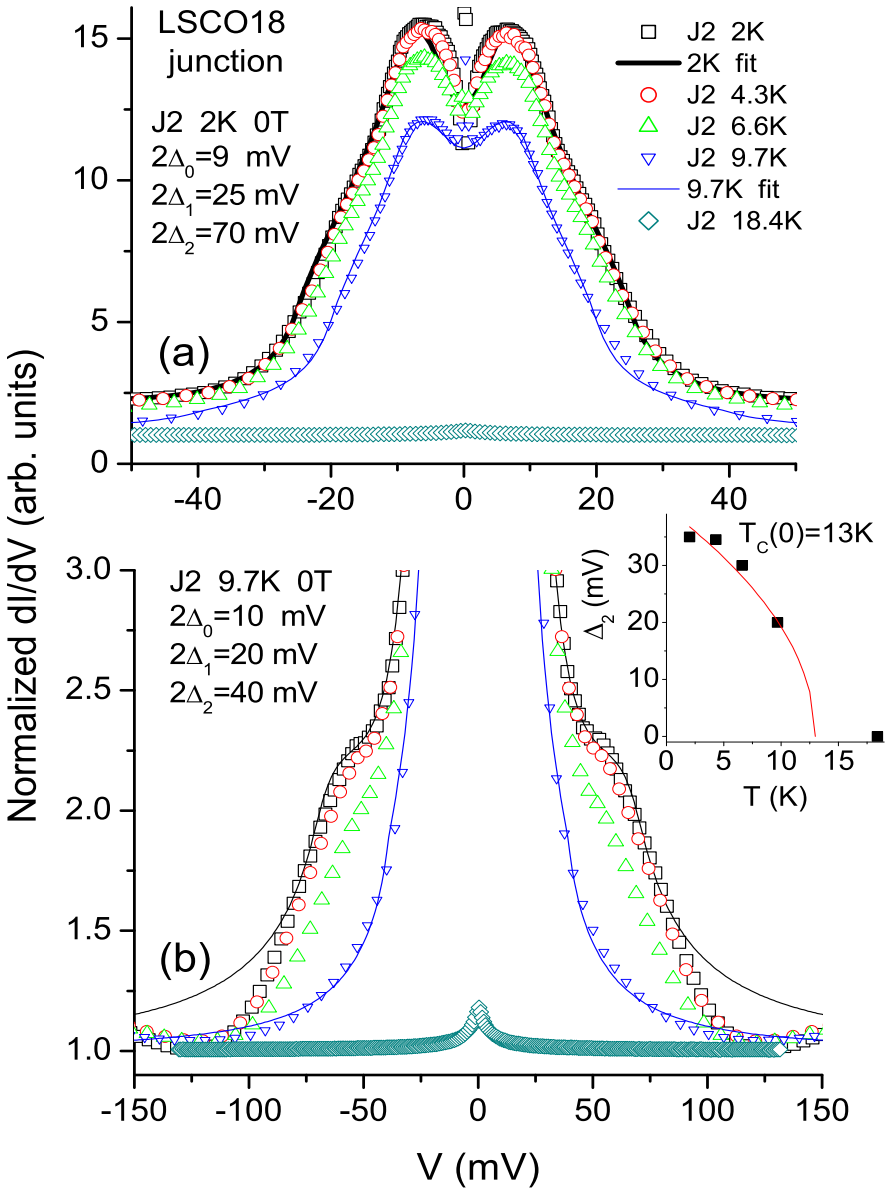

FIG. 4: Conductance spectra of the same junction as in Fig. 3 at various temperatures T at low bias 4(a), and up to high bias with zooming up on low conductances 4(b). The inset to 4(b) shows the large gap Δ_2 behavior versus T (squares) with a $\Delta_2(0)\sqrt{(T_c - T)/T_c}$ fit (line).

that $\Delta_2(T)$ behaves quite similarly to a BCS gap versus temperature, and therefore can be considered as a gap-like feature in the density of states. In addition, we found that in all junctions above T_c of both electrodes at about 30 K, all the conductance spectra were flat (not shown), which indicates that no Andreev scattering could be observed. This is in

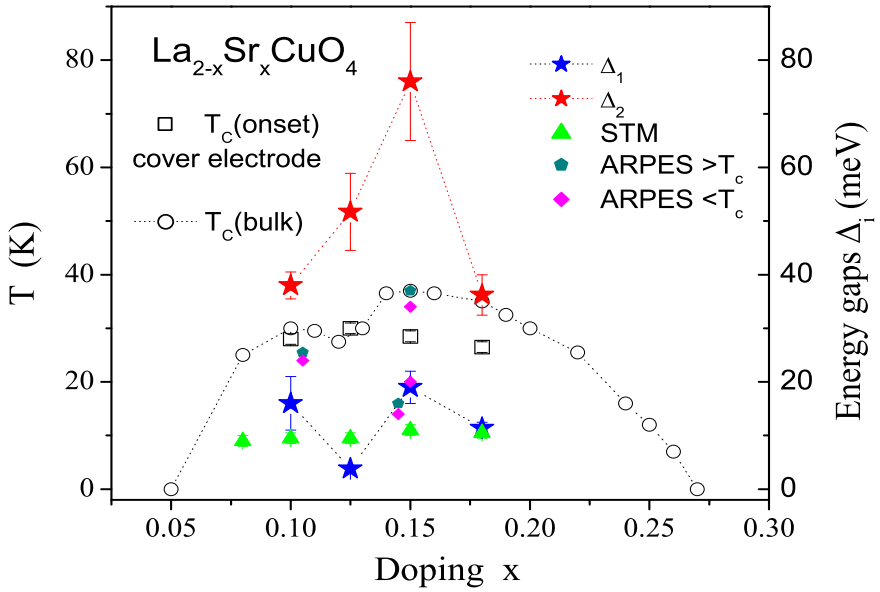

FIG. 5: The phase diagram of all the LSCOx junctions versus doping x. Shown are the bulk and cover electrode film transition temperatures, the two Andreev-like energy gaps Δ_1 and Δ_2 of the present study at 2 K, and previous STM gaps at 4.2 K [12] and ARPES gaps [4, 25, 26].

agreement with previous finding by Dagan *et al.* in NIS junctions [24]. Above T_c however, the junction contribution to the conductance is quite small compared to the significant leads resistance, and any change due to possible pairing in the pseudogap regime might be too small to be observed. Conductance spectra were also measured under magnetic fields of up to 6 T (not shown), and already at 2 T a strong suppression of all the gap-like features was observed. We thus conclude that both Δ_1 and Δ_2 represent gap-like features of the LSCOx system.

Fig. 5 summarizes on the phase diagram of LSCO the Δ_1 and Δ_2 results of the present study at 2 K versus doping. Also shown are STM and ARPES gaps [4, 12, 25, 26], and the T_c values of film and bulk LSCO [27]. The Δ_i values represent mean values of all working junctions on the wafer for each doping level and their statistical error. One can see that the general doping dependence of both Δ_1 and Δ_2 follows roughly the superconducting dome. The Δ_2 value at optimal doping of $x = 0.15$ is strongly enhanced by a factor of about

two compared the Δ_2 values at the 10% and 18% doping levels. This yields a peak-like dependence on doping of $\Delta_2(x)$ rather than a dome. The Δ_1 value is strongly suppressed at the $x = 1/8$ doping level, similar to T_c. The Δ_1 results agree with the STM observations [12], while the previous point contact results with $\Delta \approx 6 - 8$ meV [9–11] are found on the lower side of the Δ_1 values. Different ARPES gaps for LSCOx were found by different groups at x=0.145 and 0.15 doping levels. Shi *et al.* have measured Δ=14 and 16 mV well below and well above T_c, respectively [26], while the corresponding gaps that Therashima *et al.* have measured were Δ=34 and 37 mV. The former agree with our Δ_1=19±3 mV value at x=0.15 which also agrees with Yoshida *et al.* who measured $\Delta_0 \approx 20$ meV [4], but the latter as well as the ARPES gap of about 25 mV at x=0.105, fall in between the present Δ_1 and Δ_2 values. Our results thus seem to suggest that Δ_1 is the superconducting gap. Its low value at 1/8 doping also supports this conclusion if stripes are taken into account [5, 28]. Δ_2 seems to be related to T_c, since it roughly follows its doping dependence, but its origin is not so straight forward and different scenarios for it will be discussed next.

First, since the Δ_2 feature in the conductance spectra is quite small, it might be attributed to a background "step down" in the highly transparent junctions due to any excitation mode with energy $\hbar\omega$ which will appear at $eV = \hbar\omega - \Delta_1$ as discussed by Kirtley [29]. This result was obtained using a theory of inelastic transport at the junctions interface and the excitations by the tunneling or Andreev process with $\hbar\omega$ can be due to holons, bosons, phonons an so on [9, 30]. This gives symmetric spectra in agreement with the present results, but the doping dependence of Δ_2 as seen in Fig. 5 implies that these excitations have to be related to superconductivity and the way they actually do needs further theoretical treatment. A second scenario for the appearance of the Δ_2 feature is that it might be related to the Van Hove singularity (VHS) in the 2D LSCO system. Using the tt'J model it was shown that in addition to the coherence peaks at the gap energy Δ, two new and symmetric peaks appear at 2-3 times Δ in the conductance spectra due to the VHS [31]. This agrees with the present symmetric spectra and the values of Δ_2. However, when a tt't"J model was used [32], asymmetric spectra were obtained which

disagree with our results but nevertheless, the peak energies are still of the order of Δ_2. The doping dependence that follows from these results shows a monotonous increase of the energy due to the VHS feature with decreased doping, similar to the doping dependence of the pseudogap. This is in clear contradiction to our results, but in view of the fact that the calculations involved were done in attempt to explain the asymmetrical tunneling spectra of BSCO [32–34], one can not rule out that further theoretical analysis for LSCO might yield different results. Finally, although we are puzzled by the possible existence of a proper Andreev gap at such high energies as Δ_2, the reasonably good fits to our data using the d-wave BTK model [23], might indicate that Δ_2 is originated in such a gap in the density of states. To relate this to superconductivity as observed in Fig. 5, would need some bold speculation as for instance the existence of pairs with an even larger condensation energy. In this scenario then, Δ_2 will be related to Δ_1, but their relation to T_c will involve different doping dependent functions that will have to account for the fact that $\Delta_1(x = 0.15)/\Delta_1(x = 0.1) \sim 1$ while $\Delta_2(x = 0.15)/\Delta_2(x = 0.1) \sim 2$. Clearly, a thorough theoretical modelling as for the origin of Δ_2 is needed, and this might add to our understanding of the high temperature superconductors.

In conclusion, two Andreev-like energy gaps have been observed in the LSCOx cuprates, both of which scale roughly with T_c versus doping. Δ_1 is identified as the superconducting energy gap, while the origin of Δ_2 which is also related to superconductivity, is unclear at the present time and needs further theoretical modelling.

Acknowledgments: This research was supported in part by the Israel Science Foundation (grant # 1096/09), the joint German-Israeli DIP project and the Karl Stoll Chair in advanced materials at the Technion.

Supplementary material for:

Observation of two Andreev-like energy scales in $La_{2-x}Sr_xCuO_4$ superconductor/normal-metal/superconductor junctions

I. PRELIMINARY STUDIES OF S-S AND S-N RAMP-JUNCTIONS

We started the LSCO based ramp-junctions project by preparing and characterizing S-S "shorts" which are S-N-S junctions without the barrier. This was done in order to test the quality and cleanliness of our fabrication process and check the quality of the contact at the junction interface. We measured the I-V curves of LSCO10-LSCO10 shorts and extracted the critical current density at 2 K ($J_c(2K)$) by the use of the 1 μV criterion. We found that the highest values of $J_c(2K)$ ranged between $3-5\times10^6\,A/cm^2$. When compared with $J_c(2K)$ of similar LSCO10 microbridges which is typically of about $10\times10^6\,A/cm^2$, we can conclude that considering the complexity of the multi-step fabrication process of the S-S shorts [15], their quality is fairly good.

Next we prepared S-N junctions for spectroscopic characterization. We have chosen to work first with S-N junctions for two reasons. One is that having a single interface rather than two as in S-N-S junctions prevents many interference effects, and the other is that the higher resistance of the device would reduce the current density in the junction and reduce heating and non-linear effects at high bias. First we measured the resistance versus temperature of LSCO10-LSCO35 S-N junctions. We found that the low bias resistance of these junctions is in the range of 65-70 Ω, which is an order of magnitude higher than that of the corresponding S-N-S junctions (see Fig. 1 of the main paper). This leads to an order of magnitude lower current densities for the same bias (at high biases however, this changes by a factor of about 2 as can be seen in section III). Figs. 1S and 2S show the conductance spectra of two different LSCO10-LSCO35 S-N junctions on the same wafer, together with fits to the BTK model for a d-wave superconductor [23]. Although very prominent Andreev-like peaks are observed with good fits to the modified BTK model, the resulting energy gap values Δ_i are obviously much too large. Even the smallest Δ_1

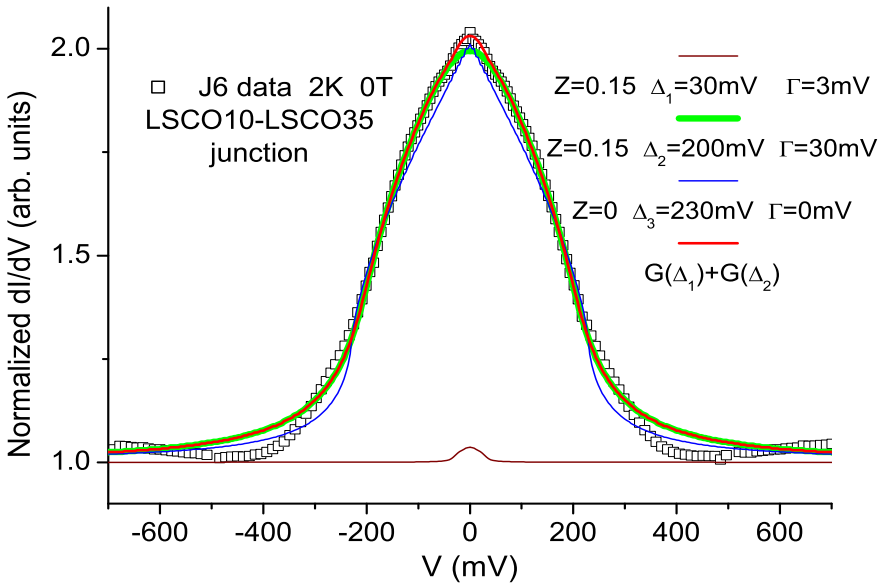

Fig. 1S: Conductance spectrum of an anti-node S-N junction of LSCO10-LSCO35 at 2K with a fit to the BTK model for a d-wave superconductor. The two components of the fit with Δ_1 and Δ_2 are shown together with a less good fit with a single gap parameter Δ_3.

values of 30 and 58 mV are much too high compared to the superconducting energy gap of LSCO10 which should be in the 10-15 mV range. The reason for these unphysically large Δ_i values is that the the voltage scale V=$V_{measured}$ in Figs. 1S and 2S is actually the sum of the voltage drop V_{lead} on the lead resistance R_{lead} of the normal LSCO35 cover electrodes (of a few mm long film from the voltage contact to the junction) and the voltage drop on the junction $V_{junction}$. To correct this problem, one has to plot the conductance versus a different V scale which is $V_{junction} = V_{measured} - V_{lead}$ as was done in Fig. 3S. Once this calibration is done, the resulting energy gap values are $\Delta_1 = 15$ mV and $\Delta_2 = 50$ mV, which agree fairly well with the corresponding values of 12-15 and 35-44 mV obtained from the conductance spectra of the S-N-S junctions (see Figs. 2 and 5 of the main paper).

In order to perform the calibration procedure as noted above, we integrated the conductance dI/dV data of Fig. 1S, and calibrated the resulting $I - V_{measured}$ curve at low bias according to the measured low bias resistance. Then the values $V_{lead} = R_{lead}I(V_{measured})$ were found, where R_{lead} was calculated from the geometry of the leads and the resistivity value of LSCO35 at 2K. This yielded the calibrated V scale $V_{junction} = V_{measured} - V_{lead}$ of Fig. 3S. The problem with this procedure is that due to the low junction resistance, this V scale depends very sensitively on the subtraction of two similar numbers $V_{measured}$ and V_{lead}, especially at low bias. Any small deviation in the value of V_{lead} due to slight thickness

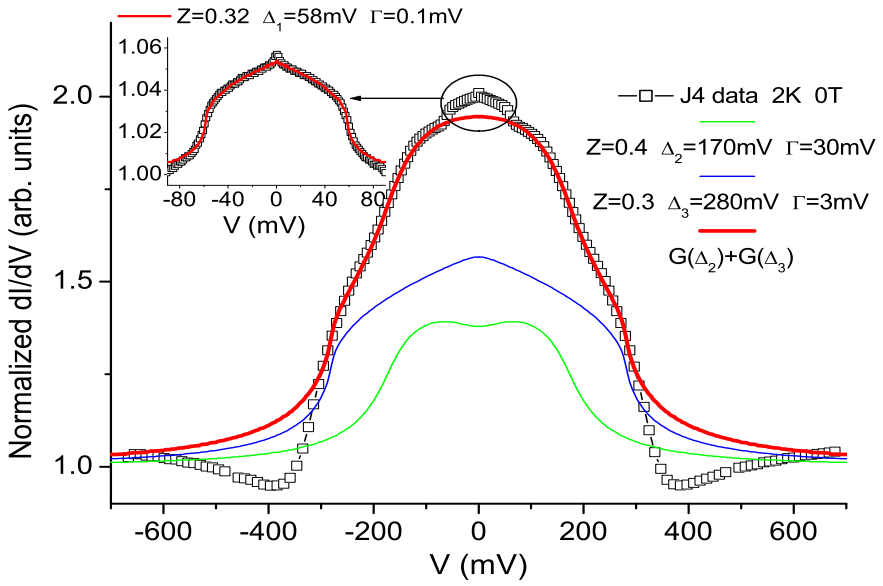

Fig. 2S: Conductance spectrum of another anti-node S-N junction of LSCO10-LSCO35 on the same wafer at 2K with a fit to the BTK model for a d-wave superconductor. The two components of the fit with Δ_2 and Δ_3 are also shown. In the inset, the low bias data in the marked circle of the main panel is fitted with a single gap value of Δ_1.

or resistivity variations on different areas of the wafer would lead to large deviations in $V_{junction}$, and sometimes even to negative values. We therefore decided that the best way to get reliable energy gap values is to use S-N-S junctions where the lead resistance is zero as long as the electrodes are superconducting. In this case, $V_{junction} = V_{measured} = V$ and all the calibration problems of S-N junctions can be avoided.

II. ADDITIONAL CONDUCTANCE SPECTRA OF LSCO15-LSCO35-LSCO15 S-N-S JUNCTIONS

In Figs. 4S, 5S and 6S we present normalized conductance spectra of the LSCO15-LSCO35-LSCO15 S-N-S junctions, which were omitted from the main paper for lack of space. These figures show three spectra with the largest, smallest and intermediate Δ_2 energy gap values, respectively. Note that this systematics of the Δ_2 values does not apply strictly to the Δ_1 values. The $2\Delta_2$ feature in Fig. 4S is observed most clearly due to the large separation between the $2\Delta_2$=220 mV and $2\Delta_1$=50 mV values. This is also seen very clearly in the second derivative data of the inset to this figure. We stress here that in

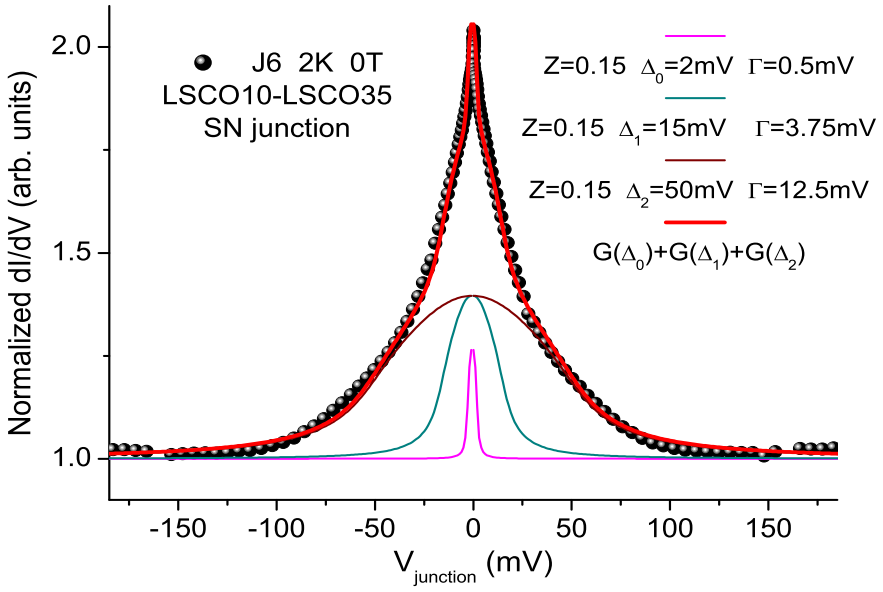

Fig. 3S: Conductance spectrum at 2K of the junction of Fig. 1 with a calibrated V scale which is the net voltage drop on the junction. A fit to the BTK model for a d-wave superconductor is also shown with its three components Δ_0, Δ_1 and Δ_2.

Fig. 5 of the main paper the Δ_2 values are mean values of all the working junctions on each wafer with their statistical errors. In the LSCO15 S-N-S junctions case there were 7 working junctions on the wafer, which yielded a mean $\Delta_2(x = 0.15)$ value of 76 mV and an error of ± 11 mV. The additional data of Figs. 4S, 5S and 6S show the robustness of the second $2\Delta_2$ feature with 0.15% Sr doping, which behaves on the phase diagram of Fig. 5 as a clear peak rather than a flat dome-like feature. We have no idea at the present time as for the origin of this behavior, except for saying that this behavior is apparently due to the optimal doping of these junctions. We can however point out the similarity between the phase diagram results of Δ_2 in Fig. 5 at 2 K and the Nernst result of T_{onset} above T_c (see Fig. 20 of Ref. [8]). Possibly, the current in our junctions decreases the phase stiffness of the condensate, leading to an uncorrelated pairs scenario similar to the one believed to occur above T_c. If this is actually the case, the relevant energy or temperature scales might be Δ_2 here, or T_{onset} in the Nernst case, respectively, but not T^* of the pseudogap.

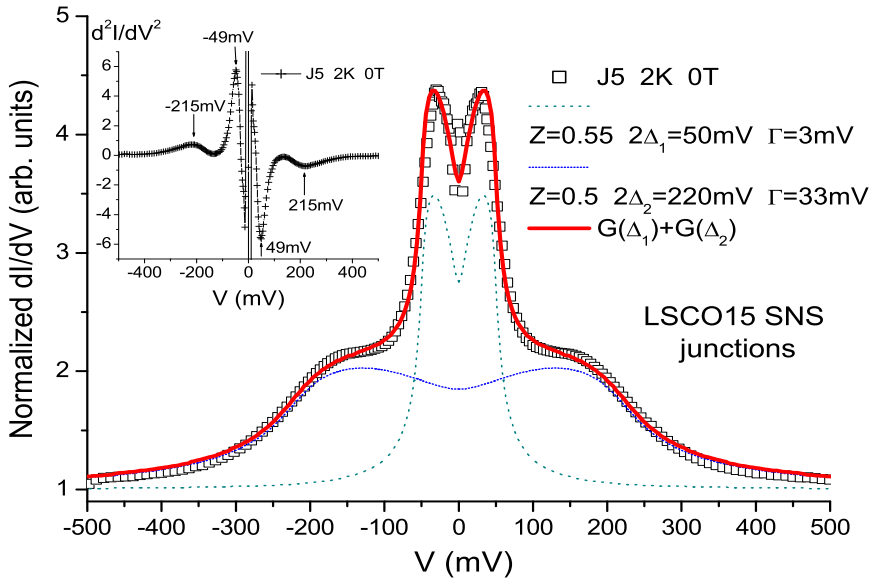

Fig. 4S: Conductance spectrum of an anti-node S-N-S junction of LSCO15-LSCO35-LSCO15 at 2K with a fit to the BTK model for a d-wave superconductor. The two components of the fit with Δ_1 and Δ_2 are also shown. The inset shows the derivative of the conductance data of this junction.

III. HIGH CURRENT DENSITY EFFECTS IN THE PRESENT STUDY

Another question that might arise concerns the high current densities at high bias used in the present study in either the S-N or S-N-S junctions. One might expect that nonlinear and heating effects play a role and that the high measuring bias current takes the junctions out of equilibrium. First, we estimate the highest critical current densities at 2 K involved in this study. In the the S-N-S junctions, the highest currents (at highest bias of 150 mV) range between 4 and 8 mA which correspond to current densities of $1 - 2 \times 10^6\, A/cm^2$. In the S-N junctions the highest currents (at highest bias of 700 mV) are of about 5-6 mA with corresponding current densities of less than $1.5 \times 10^6\, A/cm^2$. We note that the critical current density of the superconducting electrodes at 2 K is of about $10 \times 10^6\, A/cm^2$. It is thus concluded that the highest current densities in the superconducting electrodes are between 5 and 10 times smaller than the critical current density and no nonlinear or heating effects are expected. Such effects however, can still occur in the junctions and the normal electrodes. We argue that due to the very short relaxation time of the quasiparticles, on the order of the inelastic scattering time in solids which is on the order of 10^{-12} second, the system has time to relax to its equilibrium state, certainly on the time scale of the

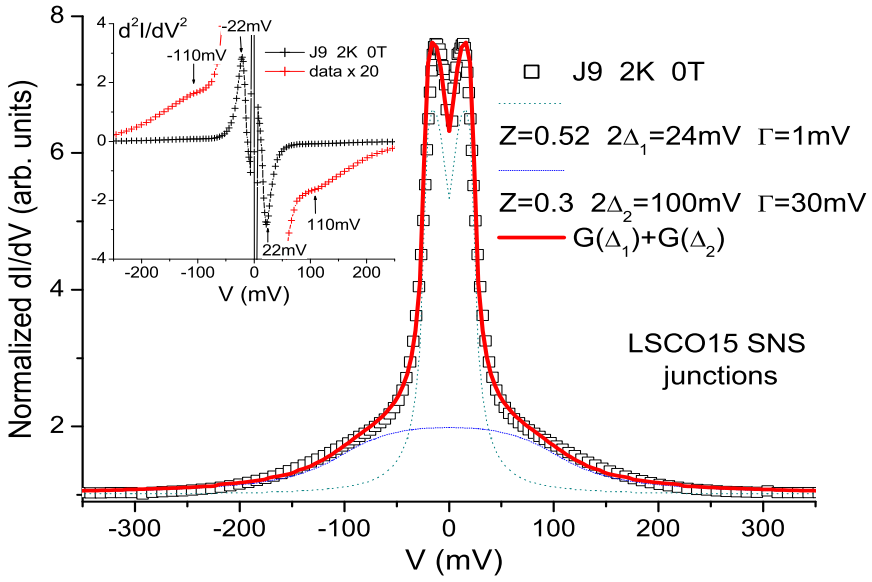

Fig. 5S: Conductance spectrum of an anti-node S-N-S junction of LSCO15-LSCO35-LSCO15 at 2K with a fit to the BTK model for a d-wave superconductor. The two components of the fit with Δ_1 and Δ_2 are also shown. The inset shows the derivative of the conductance data of this junction.

measurements which is on the order of 1 second (actually a DC measurement). Furthermore, since we measured the correct superconducting Δ_1 values at $0.5 - 1 \times 10^6\, A/cm^2$, it is hard to believe that at $1 - 2 \times 10^6\, A/cm^2$ where the Δ_2 feature was observed, a sudden change took the system out of equilibrium. In any case, Andreev spectroscopy of highly transparent junctions necessitates higher current densities than tunneling spectroscopy, so that these high current density values can not be avoided. Heating at high bias current can still be a problem. We do see some heating effects occasionally, but it is easy to detect them and stop the measurements in these cases. But the more important fact is that measurements at temperatures higher than 2 K, say at 4.3 or 6.6 K as in Fig. 4 of the main paper, show very small changes of the conductance spectra. Therefore, heating by 1-2 K at 2 K will not affect our results at all. We can thus conclude this section by saying that under the present experimental conditions nonlinear and heating effects do not play a major role.

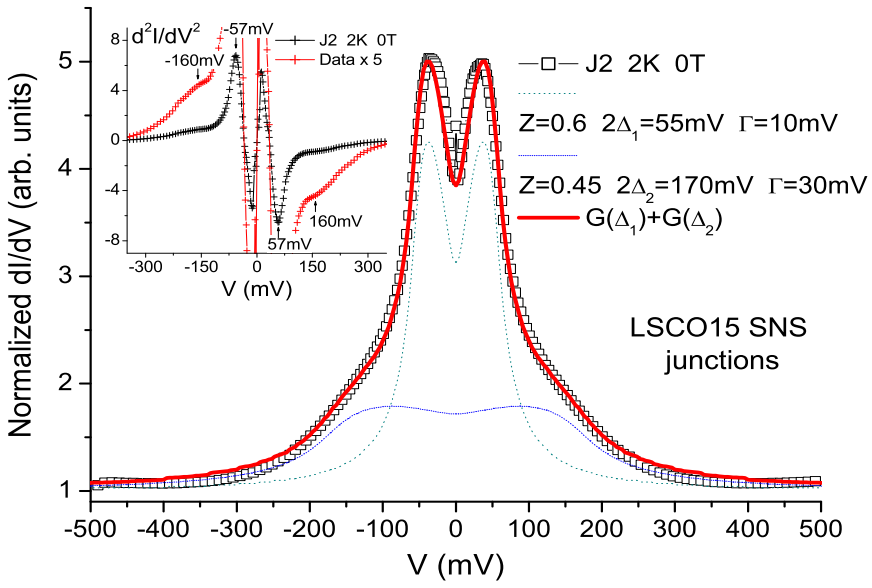

Fig. 6S: Conductance spectrum of an anti-node S-N-S junction of LSCO15-LSCO35-LSCO15 at 2K with a fit to the BTK model for a d-wave superconductor. The two components of the fit with Δ_1 and Δ_2 are also shown. The inset shows the derivative of the conductance data of this junction.

[1] Ch. Renner, B. Revaz, J.-Y. Genoud, K. Kadowaki and . Fischer, Phys. Rev. Lett. **80**, 149 (1998).

[2] G. Deutscher, Nature (London) **397**, 410 (1999).

[3] W. S. Lee, I. M. Vishik, K. Tanaka, D. H. Lu, T. Sasagawa, N. Nagaosa, T. P. Devereaux, Z. Hussain and Z.-X. Shen, Nature **450**, 81 (2007).

[4] T. Yoshida, M. Hashimoto, S. Ideta, A. Fujimori, K. Tanaka, N. Mannella, Z. Hussain, Z.-X. Shen, M. Kubota, K. Ono, Seiki Komiya, Yoichi Ando, H. Eisaki, and S. Uchida, Phys. Rev. Lett. **103**, 037004 (2009).

[5] V. J. Emery and S. A. Kivelson, Nature (London) **374**, 434 (1995).

[6] A. Kanigel, U. Chatterjee, M. Randeria, M. R. Norman, G. Koren, K. Kadowaki, and J. C.

Campuzano, Phys. Rev. Lett. **101**, 137002 (2008).

[7] U. Chatterjee, M. Shi, D. Ai, J. Zhao, A. Kanigel, S. Rosenkranz, H. Raffy, Z. Z. Li, K. Kadowaki, D. G. Hinks, Z. J. Xu, J. S. Wen, G. Gu, C. T. Lin, H. Claus, M. R. Norman, M. Randeria, and J. C. Campuzano, Nature Physics, **6**, 34 (2010).

[8] Yayu Wang, Lu Li, and N. P. Ong, Phys. Rev. B **73**, 024510 (2006).

[9] G. Deutscher, Rev. Mod. Phys. **77**, 109 (2005).

[10] G. Deutscher, N. Achsaf, D. Goldschmidt, A. Revcolevschi and A. Vietkine, Physica C **282-287**, 140 (1997).

[11] R. S. Gonnelli, A. Calzolari, D. Daghero, L. Natale, G. A. Ummarino, V. A. Stepanov, and M. Ferretti, Eur. Phys. J. B **22**, 411(2001).

[12] O. Yuli, I. Asulin, O. Millo and G. Koren, Phys. Rev. B **75**, 184521 (2007).

[13] M. Oda, N. Momono, and M. Ido, Supercond. Sci. Technol. **13**, R139 (2000).

[14] E. Polturak, G. Koren, D. Cohen, E. Aharoni, and G. Deutscher, Phys. Rev. Lett. **67**, 3038 (1991).

[15] O. Nesher and G. Koren, Phys. Rev. B **60**, 9287 (1999), O. Nesher and G. Koren, Phys. Rev. B **60**, 14893 (1999).

[16] G. Koren and N. Levy, Europhys. Lett. **59**, 121 (2002).

[17] J. P. Locquet, J. Perret, J. Fompeyrine, E. Machler, J. W. Seo and G. Van Tendeloo, Nature **394**, 453 (1998).

[18] M. Tinkham, *Introduction to superconductivity*, pp 77, McGraw-Hill, New York (1996).

[19] W. J. Tomasch, Phys. Rev. Lett. **15**, 672 (1965); 16, **16** (1966).

[20] J. M. Rowell and W. L. McMillan, Phys. Rev. Lett. **16**, 453 (1966).

[21] O. Nesher and G. Koren, Appl. Phys. Lett. **74**, 3392 (1999).

[22] See supplementary material starting on page 11 here for additional conductance spectra of SN and SNS junctions of the LSCOx-LSCO35 system.

[23] Y. Tanaka and S. Kashiwaya, Phys. Rev. B **53**, 9371 (1996).

[24] Y. Dagan, A. Kohen, G. Deutscher, A. Revcolevschi, Phys. Rev. B **61**, 7012 (2000).

[25] K. Terashima, H. Matsui, T. Sato, T. Takahashi, M. Kofu, and K. Hirota, Phys. Rev. Lett. **99**, 017003 (2007).

[26] M. Shi, J. Chang, S. Pailhes, M. R. Norman, J. C. Campuzano, M. Mansson, T. Claesson, O. Tjernberg, A. Bendounan, L. Patthey, N. Momono, M. Oda, M. Ido, C. Mudry, and J. Mesot,

Phys. Rev. Lett. **101**, 047002 (2008).

[27] T. Matsuzaki, M. Ido, N. Momono, R. M. Dipasupil, T. Nagata, A. Sakai,and M. Oda, J. Phys. Chem. of Solids **62**, 29 (2001).

[28] H. Sato, A.T sukada, and M. Naito, Physica C **408-410**,848 (2004).

[29] J. R. Kirtley, Phys. Rev. B **47**, 11379 (1993).

[30] P. W. Anderson, and Z. Zou, Phys. Rev. Lett. **60**, 132 (1988).

[31] A. J. Fedro, and D. D. Koelling, Phys. Rev. B **47**, 14342 (1993).

[32] B. W. Hoogenboom, C. Berthod, M. Peter, and O. Fischer, and A. A. Kordyuk, Phys. Rev. B **67**, 224502 (2003).

[33] T. C. Ribeiro, and X. G. Wen, Phys. Rev. Lett. **97**,057003 (2006).

[34] G. L. de Castro, C. Berthod, A. Piriou, E. Giannini, and O. Fischer, Phys. Rev. Lett. **101**, 267004 (2008).